THE JOURNAL OF PHYSICAL CHEMISTRY B

Article

pubs.acs.org/JPCB

Cavity Closure Dynamics of Peracetylated β-Cyclodextrins in Supercritical Carbon Dioxide

Muhannad Altarsha, Francesca Ingrosso,* and Manuel F. Ruiz-López*

Equipe de Chimie et Biochimie Théoriques, SRSMC, University of Lorraine, CNRS, BP 70239, 54506 Vandœuvre-lès-Nancy Cedex, France

Supporting Information

ABSTRACT: Structural properties of peracetylated β-cyclodextrin in supercritical carbon dioxide were investigated by means of molecular dynamics simulations. The study indicated a strong reduction of the cavity accessibility to guest molecules, compared to native β-cyclodextrin in water. Indeed, the cavity is self-closed during the largest part of the simulation, which agrees well with suggestions made on the basis on high-pressure NMR experiments. Self-closure happens because one glucose unit undergoes a main conformational change (from chair to skew) that brings one of the acetyl groups in the wide rim of the cyclodextrin to the cavity interior. This arrangement turns out to be quite favorable, persisting for several nanoseconds. In addition to the wide rim self-closure, a narrow rim self-closure may also occur, though it is less likely and exhibits short duration (<1 ns). Therefore, the number of solvent molecules reaching the cavity interior is much smaller than that found in the case of native β-cyclodextrin in water after correction to account for different molar densities. These findings support the weak tendency of the macromolecule to form host−guest complexes in this nonconventional medium, as reported by some experiments. Finally, Lewis acid/base interactions between the acetyl carbonyl groups and the solvent CO_2 molecules were analyzed through ab initio calculations that revealed the existence of a quite favorable four-member ring structure not yet reported. The ensemble of these results can contribute to establish general thermodynamic principles controlling the formation of inclusion complexes in supercritical CO_2, where the hydrophilicity/hydrophobicity balance is not applicable.

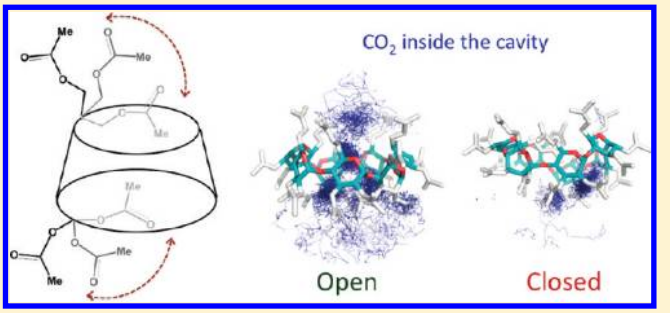

I. INTRODUCTION

Cyclodextrins (CDs) are cyclic macromolecules formed by monosaccharide (glucopyranose) units linked together through 1−4 bonds.[1] They occur in nature in native forms with six (α-CD), seven (β-CD), or eight (γ-CD) units, and have become extremely important in the past years due to their versatile properties.[2] Native cyclodextrins are soluble in water and display a relatively rigid half-cone shape with a hydrophobic internal cavity where low polar molecules can be trapped, thus improving their solubilization. The glucopyranose units exhibit a $^4C_1$ chair conformation and lie in a *syn* orientation with respect to the glycosidic linkages. This results in a structure having one primary −OH group per glucose unit on the narrow side and two secondary −OH groups per glucose unit on the wide side. For instance, native β-CD (N-β-CD), the most common natural CD, has 7 primary and 14 secondary hydroxyls (Figure 1).

The marked CDs ability to form host−guest complexes is well documented and has been widely exploited by the pharmaceutical industry to improve the bioavailability of drugs. The β-CD macrocycle is particularly interesting from this point of view owing to its suitable cavity size.[3−5] Functionalization of the hydroxyl groups has been envisaged to change the CD properties,[1,6−8] and understanding the associated structure/activity relationships has become an extremely important objective in drug design.[5,7,9,10]

Recently, the use of supercritical CO_2 ($scCO_2$) has attracted attention for the preparation of drug−CD inclusion complexes (for a review, see ref 11 and references cited therein). Indeed, the development of supramolecular chemistry in $scCO_2$ is an exciting field that has a great potential industrial interest since $scCO_2$ is very promising as a solvent in the context of green chemistry. Carbon dioxide is inexpensive, nonflammable, and nontoxic and has a much lower impact on the environment than the usual volatile organic solvents.[12−16] In addition, $scCO_2$ involves mild temperature and pressure conditions and can be easily separated from the dissolved compounds by decompression.[17,18] Interestingly, it has been used as an efficient reaction medium to synthesize β-CD derivatives by means of the Staudinger−Aza−Wittig reaction,[19,20] where CO_2 is also a reactant.

A major shortcoming in this field is the insolubility of N-β-CD in $scCO_2$, although experimental work[21−23] has shown the high solubility of the peracetylated derivatives (PA-β-CD). This

Received: January 4, 2012
Revised: February 22, 2012
Published: March 3, 2012

dx.doi.org/10.1021/jp3001064 | J. Phys. Chem. B 2012, 116, 3982−3990

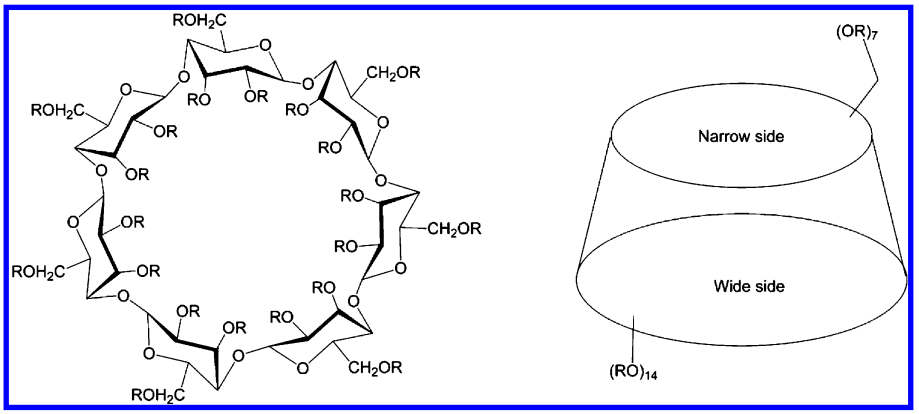

Figure 1. Schematic representation of β-cyclodextrins (in the native form, R = H).

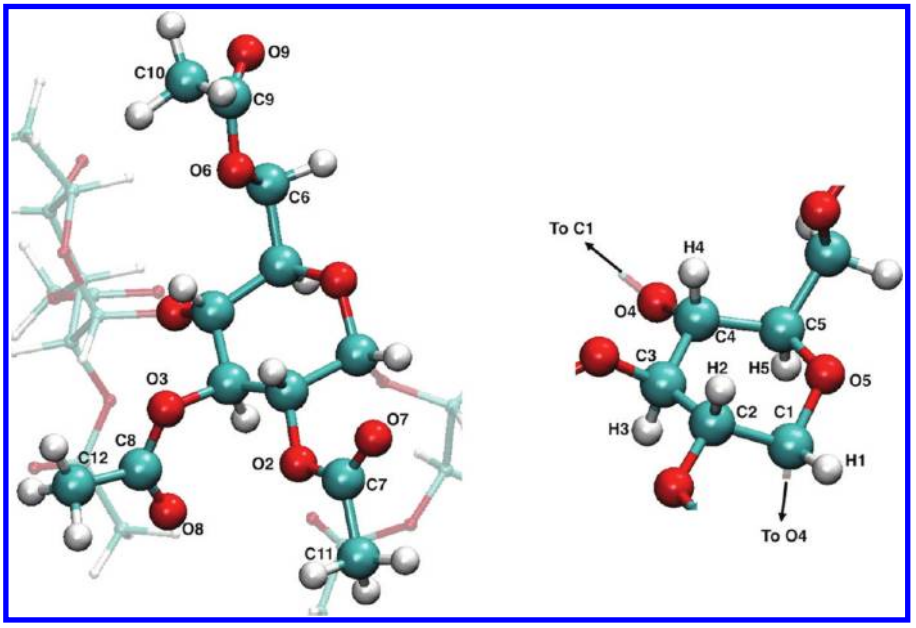

Figure 2. Atom labels for a glucopyranose unit in the peracetylated β-CD studied in this work (R = $COCH_3$ in Figure 1).

has been attributed to the acid/base Lewis interaction between carbonyl groups and solvent CO_2 molecules.[24,25] It is now established, on the other hand, that the half-cone structure of CDs is largely perturbed by acetylation of the hydroxyl groups. Thus, distortions of peracetylated β-CDs have been reported in the solid state[26] and in organic solvents ($CDCl_3$ and CD_3OD).[27] X-ray crystallographic data showed also main changes of the PA-γ-CD structure[28] and of permethylated α-, β-, and γ-CDs.[29] Such modifications may of course affect the ability of the macrocycles to form host−guest complexes, but this essential question has not been sufficiently explored yet.

Galia et al.[30] monitored the interaction between triphenylphosphine derivatives with PA-β-CD in $scCO_2$ using UV−visible spectroscopy. The authors observed the formation of inclusion complexes but obtained much smaller complexation constants than those found in water (by 1−3 orders of magnitude). The result was attributed to the absence of hydrophobic effects, the CO_2-phobic effect being weaker. However, further work by the same group[31] showed a modest increase of the inclusion constant after addition of 9 mol % methanol, which led the authors to modify their first hypothesis. They deduced that the effect is rather connected with the distortion of the cyclic oligosaccharide conformation.

A similar conclusion was reached by Ivanova et al.[32] from their high-pressure NMR investigation of PA-β-CD in $scCO_2$. The results of the NOE studies were consistent with a change of the glucose unit from the chair to the skew-boat conformation though the data did not allow determining the number of glucose residues that undergo such an alteration. On the other hand, the detected NOE contacts indicated that some acetyl groups are directed toward the inside of the cavity, in both the narrow and the wide sides. Hence, the authors hypothesized a self-closure of the cavity that was also supported by the nonexistence of inclusion complexes with captopril and flufenamic acid. The data indicated, nevertheless, an enhanced solubility of captopril in $scCO_2$ in the presence of the acetylated CD, so that some interactions between the host and the guest probably exist.

From the theoretical point of view, PM3 calculations were performed for the inclusion complex of PA-β-CD with diphenyl(4-phenylphenyl)phosphine in the gas phase.[33] The study predicted the formation of a stable complex but such conclusions must be regarded with circumspection due to the well-known limitations of the semiempirical PM3 method in describing intermolecular interactions,[34−36] in particular in CD inclusion complexes.[37] Many theoretical studies have been

dx.doi.org/10.1021/jp3001064 | J. Phys. Chem. B 2012, 116, 3982−3990

devoted to study the structure of CDs in water (see, for instance, refs 38−44) but to our knowledge, so far no theoretical work has analyzed their properties in $scCO_2$.

With the aim of getting a deeper insight into this topic, we report here a study of PA-β-CD in $scCO_2$, based on classical molecular dynamics simulations and ab initio calculations. Our intent is to provide a theoretical analysis of some fundamental properties, not yet addressed in the studies mentioned above, and which will be difficult to be achieved experimentally. We focus on (1) the structure of CD, specifically the number of glucose units undergoing conformational changes and the nature of these changes; (2) the degree of cavity self-closure and cavity accessibility to solvent (and potentially to guest molecules); (3) the dynamics of acetyl groups in solution and the oscillation (if any) between open and closed cavity shapes; and (4) the nature of solute−solvent interactions.

II. COMPUTATIONAL METHODS

We run classical molecular dynamics simulations using the sander code in Amber9.[45] The potential used to describe the solvent was the one developed for the EPM2 model.[46] It has been shown that this potential reproduces the liquid−vapor coexistence curve and the critical properties of the CO_2 fluid. In particular, the critical temperature T_c is 304 K, and the critical density 468.0 kg/m^3, reproducing the corresponding experimental values.[21] As for the solute, we used the Glycam force field,[47,48] though the model charges for the acetyl groups had to be parametrized, since they were not included in the original force field. To evaluate such model charges, the procedure had to be made consistent with the Glycam parameters. To this aim, we considered a single glucopyranoside unit in which the oxygen atoms O4 and O5 were methylated, and O2, O3, and O6 acetylated (see Figure 2 for atom labels in glucopyranose units). After geometry optimization at the Hartree−Fock 6-31G(d)+ level, we adopted the RESP[49,50] procedure to calculate partial charges, by keeping the already available Glycam charges fixed, and optimizing the ones corresponding to the acetyl groups by imposing the neutrality of the molecule. The Gaussian 09 program was used for charge calculations and geometry optimizations.[51] The charges were calculated at the same quantum level at which the geometry optimization was performed, and the results are reported as Supporting Information.

Simulations were run at the thermodynamic conditions corresponding to a solution having a concentration of 5 wt % in the cyclodextrin, a pressure of 40 MPa, and a temperature of 313 K, using a cubic simulation box with periodic boundary conditions (the simulation box size was L = 77.75 Å, and CD molecule was immersed in 4356 CO_2 molecules). The Ewald method[52] was used for the long-range electrostatics, and a cutoff radius of 10 Å was used for nonbonded interactions. Equilibration was run in the NPT ensemble for 5 ns, followed by 2 ns in the NVE ensemble. The analysis was performed on a 10 ns simulation in the NVE ensemble.

Simulations of N-β-CD in water were also performed, using the conditions described before.[53] The CD was modeled using the Amber03 force field[54] and immersed in TIP3P water.[55] Simulations for one N-β-CD immersed in 4955 water molecules in a parallelepipedal box (dimensions 53.24 × 59.12 × 60.32 Å^3) were run in the NVT ensemble (T = 300 K) with periodic boundary conditions and the particle mesh Ewald method[56] to deal with long-range electrostatics. The figures have been prepared using the programs VMD[57] and Pymol.[58]

III. RESULTS AND DISCUSSION

A. Glucopyranose Units Conformation. As said in the introduction of the paper, experimental work has indicated important distortions of the cavity in peracetylated cyclodextrins. The most striking result in our simulations of PA-β-CD in $scCO_2$ is the existence of a chair-to-skew conformational change in one (and only one) of the seven glucopyranose units. This is in contrast with the behavior of N-β-CD in water, where each unit remains stable in a chair conformation. For isolated glucose units, metadynamics simulations within the Car−Parrinello approach predict barriers between different conformations that can be as high as 10 kcal/mol.[59] However, the conformational free energy landscape of the glucopyranose units in PA-β-CD is modified by steric interactions between the acetyl groups and by the macrocavity geometrical constraints. As mentioned above, the results obtained by NMR and crystallography experiments hint at a PA-β-CD cavity with a glucopyranose unit in the skew conformation. In other words, the process leading from PA-β-CD with seven units in chair conformation to PA-β-CD with six units in chair and one in skew conformations is exoergic and therefore it probably has a much lower activation barrier than the chair-to-skew process in an isolated glucopyranose unit.

The ring's conformation can be characterized by looking at the values of the O5−C5−C4−C3 and O5−C1−C2−C3 dihedral angles as a function of time (see Figure 2 for the labels used to identify the atoms). The analysis is reported in Figures 3 and 4. Figure 3 shows the time evolution for the unit subject

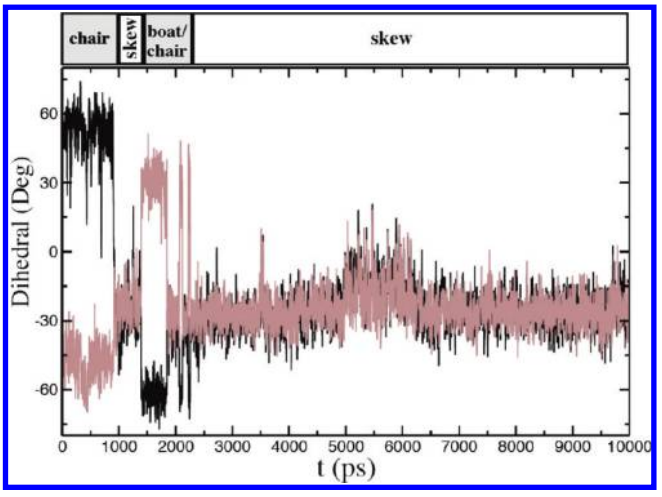

Figure 3. Time evolution of the O5−C5−C4−C3 (brown line) and O5−C1−C2−C3 (black line) dihedral angles for one of the seven glucopyranose units in the PA-β-CD macrocycle subject to conformational changes.

to conformation changes. In a large portion of our simulation, this unit is in a skew conformation. The chair conformation is present only in a small time window at the beginning of the simulation (first nanosecond). Another chair structure, not equivalent to the first one, appears between 1.5 and 2.5 ns. Some extremely short transitions to boat are also observed. Figure 4 displays the dihedral angle histograms for the other units; we compare them to the corresponding quantities for N-β-CD in water. The values reveal that these units stay in a chair conformation during all the simulation time, though they seem more flexible than in N-β-CD in water.

dx.doi.org/10.1021/jp3001064 | J. Phys. Chem. B 2012, 116, 3982−3990

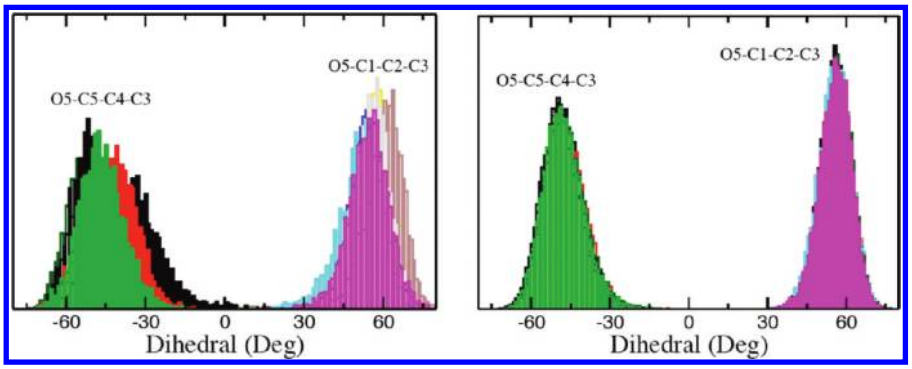

Figure 4. Distribution of dihedral angles for PA-β-CD in $scCO_2$ (left) and for N-β-CD in water (right). In the former case, we do not include the distribution for the unit in which chair-to-skew conformational change is observed, shown in Figure 3.

These results are consistent with the experimental findings of Ivanova et al.[32] The authors reported that the most likely explanation to the observed NOE spectra of PA-β-CD in $scCO_2$ can be related to a chair to skew ring inversion. Indeed, when the units are in a chair conformation, all the acetyl groups occupy equatorial positions with respect to the sugar ring, while the inversion to the skew conformation involves a rearrangement that is schematized in Figure 5. Acetyl groups on the wide

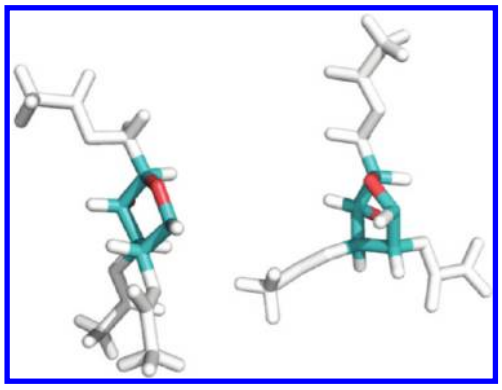

Figure 5. Chair (left) vs skew (right) conformations of a glucopyranose unit in PA-β-CD illustrating the different positions of the acetyl groups (gray color) in each case: all groups occupy the equatorial positions in the chair conformation, while two of them are in pseudoaxial positions in the skew conformation.

side change from equatorial to pseudoaxial positions (and correspondingly, two H atoms change from axial to pseudoequatorial position). The acetyl group on the narrow side stays in an equatorial position. Formally, when these conformational changes occur, the description of the CD macrocycle as a truncated cone is no longer appropriate. However, for the sake of simplicity we shall continue to use the terms wide and narrow sides in the rest of paper.

B. Macrocycle Self-Closure. The rearrangement of the acetyl groups when the skew conformation is formed has important consequences in terms of the CD cavity accessibility, as can be inferred from the structures drawn in Figure 6. The acetyl group attached to the C3 atom points toward the CD exterior, whereas the one attached to the C2 atom points toward the CD interior and hinders the cavity. This leads to a CD macrocycle self-closure on the wide side and agrees with previous suggestions made on the basis of NMR data.[32]

The self-closure of the CD cavity at the wide side is not, however, the only structural consequence induced by the

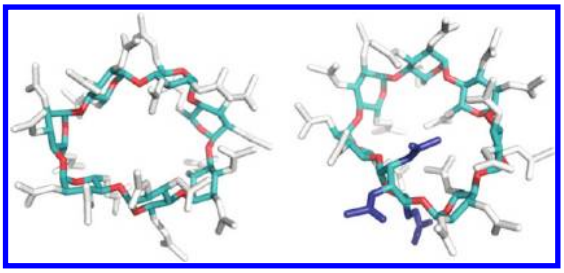

Figure 6. Snapshots showing two different types of PA-β-CD structures (views from the wide side) and the position of the acetyl groups (in gray or deep blue). Hydrogen atoms are not shown for clarity. Left: all glucopyranose units are in the chair conformation. Right: one unit has switched to a skew conformation (associated acetyl groups in deep blue). In the former case, the CD cavity is easily accessible, whereas in the latter case one of the acetyl groups on the wide side enters the cavity, rendering the overall structure more distorted and the cavity less accessible.

adoption of a skew conformation by one glucopyranose unit. Indeed, one of the adjacent units (the one linked to the O4 atom), undergoes significant distortions, with large-amplitude motions of the corresponding acetyl groups. Occasionally, the acetyl group on the narrow side clearly enters the CD cavity. To monitor such an event type, we calculated the distance r between the C10 atom of the implicated acetyl group and the CD center of mass (c.o.m.) as a function of time. Different choices were examined to determine a point representative of the cavity center, since the CD structure is strongly deformed during the simulation. By visualizing the position of the cyclodextrin center of mass along the trajectory, we decided that this is reasonably close to the position of cavity center.

In Figure 7, we show the results thus obtained. At the beginning of the simulation, the acetyl group is oriented toward the CD exterior and hence it is far from the center of the cavity ($r \approx 10$ Å). During that time period, all the glucopyranose units are in the chair conformation and, as said above, the CD cavity is fully accessible on both sides. At about $t = 1$ ns (i.e., when the first chair-to-skew conformational change is observed, see Figure 3), the acetyl group reorients abruptly and enters the cavity ($r \approx 1$ Å). When this occurs, the CD cavity is self-closed in both the narrow and wide sides (see snapshot in Figure 7). Such a situation remains for about 0.5 ns but similar events are again observed at about 5−6 and 8 ns (note that we never observe the acetyl group on the narrow side going back to the initial position, i.e., oriented outward, which can be explained by the fact that the initial CD structure with all units in the chair conformation is never recovered along the simulation).

dx.doi.org/10.1021/jp3001064 | J. Phys. Chem. B 2012, 116, 3982−3990

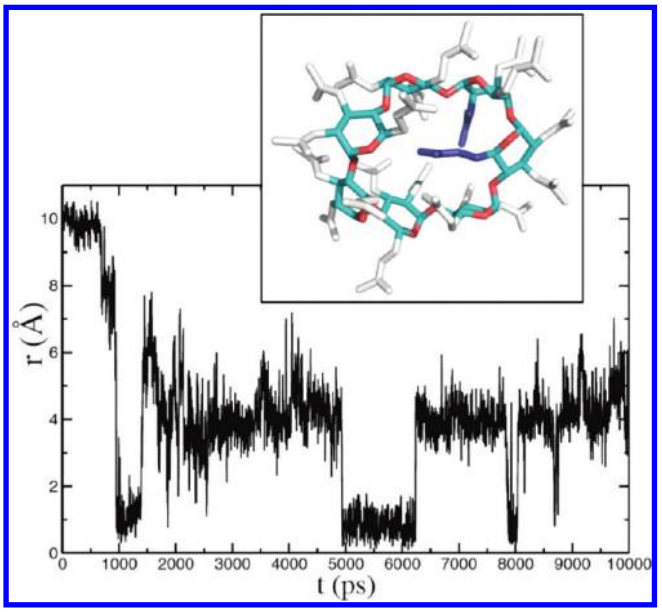

Figure 7. CD cavity self-closure on the narrow side: r corresponds to the distance between the C10 atom of the monitored acetyl group and the CD center of mass. The monitored acetyl group (see text) belongs to a glucopyranose unit (narrow side) that is adjacent to the skewed one and linked to it through the O4 atom. The snapshot at t = 6000 ps illustrates the case of a cavity closed by two acetyl groups (deep blue) on the wide and narrow sides (hydrogen atoms are not shown for clarity).

In summary, our simulations are indicative of PA-β-CD cavity self-closure on both the wide and narrow sides. In the first case, the process results from a chair-to-skew conformational change undergone by one of the glucopyranose units. In the second case, the process is indirectly induced by this conformational change but it involves an acetyl group of the adjacent glucose unit. Self-closure on the wide side is present for most of the simulation time while self-closure on the narrow side occurs for relatively short time periods (<1 ns).

C. Cavity Accessibility to the Solvent. As suggested by the results presented above, the accessibility of the PA-β-CD cavity to form inclusion complexes seems very limited. In fact, NMR measurements for two pharmaceutical compounds, captopril and flufenamic acid,[32] showed the nonexistence of inclusion complexes with PA-β-CD. Though host−guest complexes were not considered in our study, we investigated the accessibility of the PA-β-CD cavity to solvent molecules. To this purpose, we calculated the radial distribution function (RDF) of solvent CO_2 molecules with respect to the cyclodextrin center of mass and compared the results to the equivalent calculation for N-β-CD in water. The results are shown in Figure 8. It is important to stress that when making this comparison one should keep in mind the different molar densities of the two solvents. In our simulation conditions, the molar density of water is 0.055 mol/cm^3 while that of $scCO_2$ is 0.015 mol/cm^3 (corresponding to about 1.45 times the critical density of the fluid). Thus, the molar density of liquid water is about 4 times that of $scCO_2$.

Integration of the RDFs in $scCO_2$ to evaluate the average number of solvent molecules N within the cavity leads to about N = 0.7 molecules (using either the C or the O curves and limiting the integration to r = 6 Å). In the case of N-β-CD in water, we find 8 solvent molecules, which is in reasonably good agreement with other simulations and experimental work in the literature,[40,41,44] where this number was evaluated to be between 5 and 7. On average, therefore, the number of CO_2 molecules included in the CD cavity is much smaller compared to that of water molecules, even after correction to take into account the different molar densities of the two solvents.

The general conclusion that we can draw from these results is the confirmation of the experimental observation that, on average, the PA-β-CD cavity exhibits a low accessibility; nevertheless, further analysis of this property is interesting. We report in Figure 9 the RDFs obtained along three time periods of 150 ps, during which the cavity displays a different shape, open (region I), closed (region II), and partially closed (region III). For each region, we sampled the trajectory with a higher frequency compared to the long simulation run (saving the coordinates of the system each 3 fs, to be compared with saving each 3 ps in the overall 10 ps long run). By comparing the curves in Figure 8 (left panel) and in Figure 9, we can notice that the average over the full 10 ns trajectory is just a blurred picture of a structure undergoing many dynamical changes. In region I (open cavity) and region III (partially closed cavity), the integrated number of solvent molecules is similar, N = 2, and much larger than the global average (as before, the integration is done up to r = 6 Å). The peaks in these two regions present, however, significant differences; note in particular the fact that in region III their intensity goes to zero at roughly r = 2.5 Å. In region II (closed cavity), no peak at short distances (0−2 Å) has been found. The first peak in this case appears at r close to 4 Å, indicating that solvent molecules cannot get close to the cavity center. The integrated number of solvent molecules is now below the global average, N = 0.5.

To help interpreting these results, we tracked the position of those C atoms of the CO_2 molecules lying within 10 Å from the

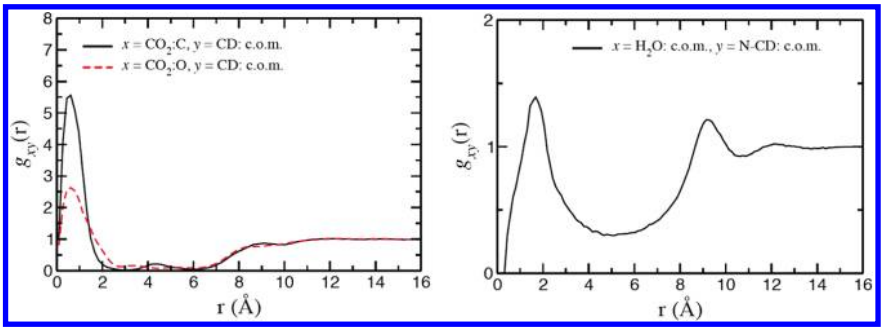

Figure 8. Radial distribution functions of solvent molecules around the CD center of mass for PA-β-CD in $scCO_2$ (left) and N-β-CD in water (right).

dx.doi.org/10.1021/jp3001064 | J. Phys. Chem. B 2012, 116, 3982−3990

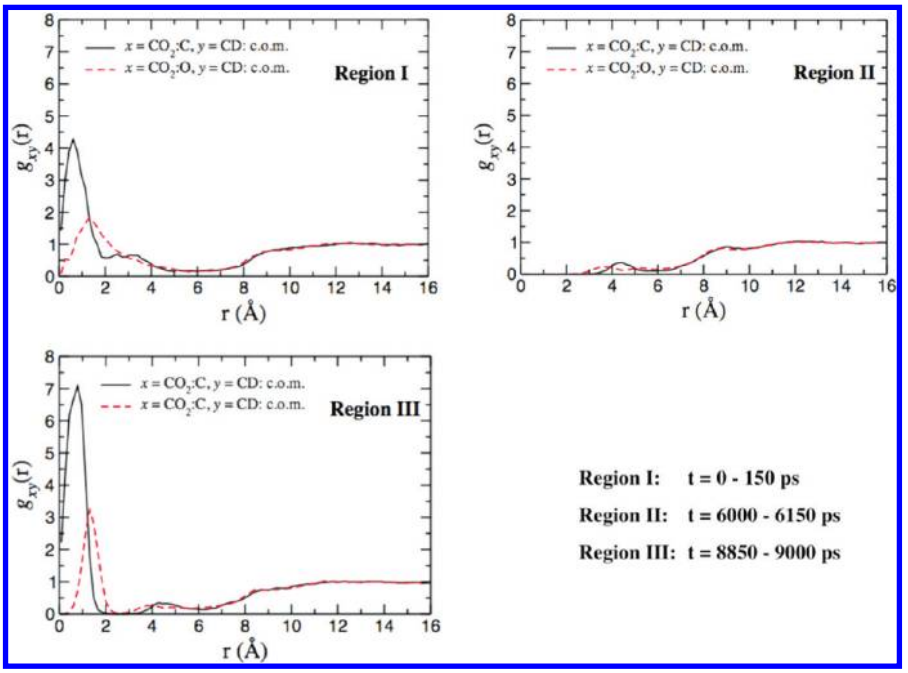

Figure 9. Radial distribution functions for C and O solvent atoms with respect to the CD center of mass for PA-β-CD in $scCO_2$. Three different time periods extracted from the whole simulation are displayed, showing the strong time dependence of solvent molecules inclusion into the CD cavity.

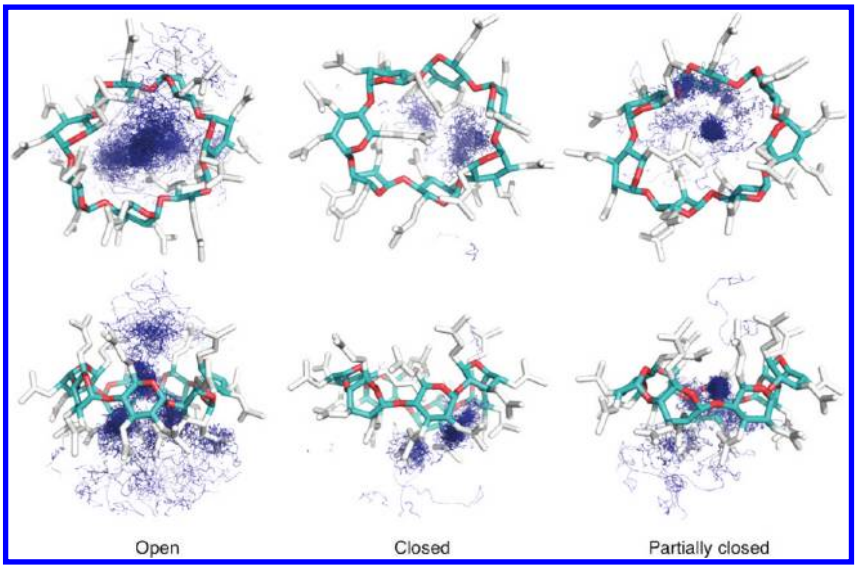

Figure 10. Trace of the carbon atom of the CO_2 solvent molecules nearby the CD c.o.m. (see text). Top and side views are presented for the three different regions of our simulation described in Figure 9, corresponding to CD cavity open (region I), closed (region II), and partially closed (region III). A representative CD conformation is drawn for clarity (hydrogen atoms are not shown for clarity).

CD center of mass. We repeated the same analysis for the three 150 ps long subtrajectories (to simplify, we retained only the solvent molecules that stay within a distance of 6 Å for at least 5% of the overall time in the subtrajectory). At each time step, we defined an internal reference system whose axes are parallel to the CD inertial axes. In Figure 10, we report pictures corresponding to the three time periods considered above. As shown, only when the cavity is totally (region I) or partially (region III) open, the density of CO_2 molecules is significant near the center of the cavity. In region II, the solvent density appears to be concentrated on one side of the cavity, in an opposite position with respect to the closing acetyl groups. Noticeably, only in region I the CO_2 molecules are reasonably free to move within the cavity and to diffuse to the exterior. In region II and to a lesser extent in region III, the solvent molecules appear to be more confined; i.e., the exchange between the interior and the exterior is impeded.

D. Solute–Solvent Interactions. The solubility of PA-β-CD in $scCO_2$ is thought to be due to the CO_2-philic character of the acetyl groups. To examine this point, we turn now to analyzing solute–solvent interactions, and in particular the existence of possible specific interactions between the solvent and the acetyl groups. First of all, we present the radial distribution function (RDF) between the carbonyl oxygen atoms of the three acetyl groups in the CD and the carbon and oxygen atoms of the solvent (see Figure 11). Both on the narrow and on the wide side, a well-defined peak around 3 Å is observed in the $O\cdots C_{solvent}$ RDFs, and at slightly larger

dx.doi.org/10.1021/jp3001064 | J. Phys. Chem. B 2012, 116, 3982–3990

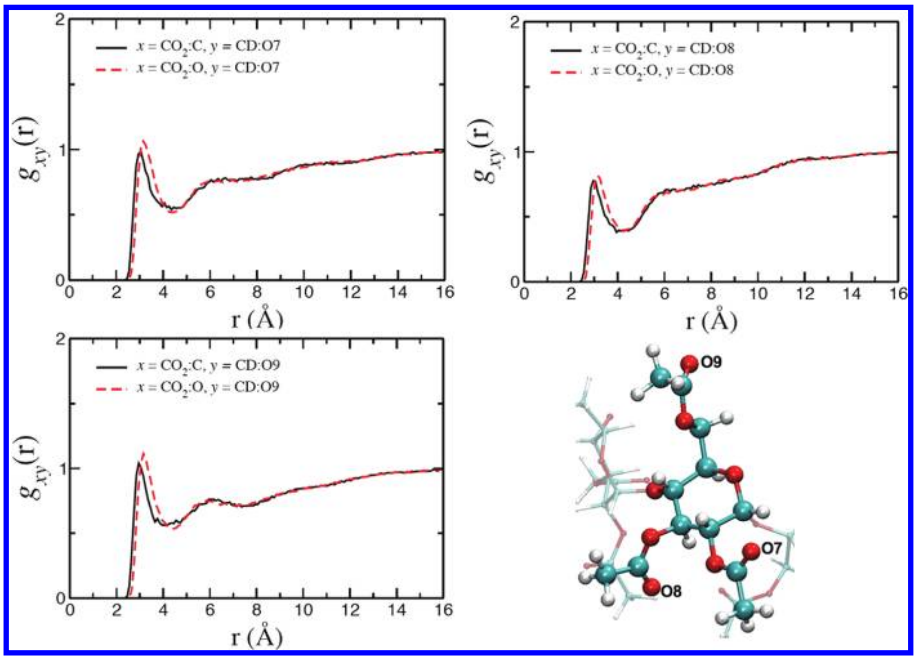

Figure 11. Solute−solvent radial distribution functions for the C and O atoms of the solvent around the carbonyl O atoms (acetyl groups) on the narrow (O9) and on the wide (O7 and O8) side of PA-β-CD in $scCO_2$.

distances in the corresponding $O\cdots O_{solvent}$ distributions, confirming the existence of specific solute−solvent interactions. Our results are consistent with the expected Lewis acid character of the CO_2 molecule, and the predicted average $O\cdots C_{solvent}$ intermolecular distances (3.0 Å) are comparable to the distance found by performing ab initio calculations for methyl acetate−CO_2 interactions in the gas phase (≈2.84 Å).[60,61] In those studies, it was suggested that the CO_2 molecule may also cooperatively interact with the methyl hydrogen atoms, as represented in Scheme 1 (N.B., the O═C—C—H dihedral angle is 11.7° in the structure corresponding to the energy minimum[61]). However, such an $H\cdots O_{solvent}$ interaction was estimated to be very weak (about 0.2 kcal/mol). The total interaction energy is about −3.4 kcal/mol at the highest calculation levels.[60,61] The results obtained in our simulations seem to confirm the weakness of this interaction, since the $H\cdots O_{solvent}$ RDFs display only broad, low-intensity features at distances corresponding to the first solvation shells (see Figure 12).

Scheme 1. Structure Proposed before for the Methyl Acetate−CO_2 Complex

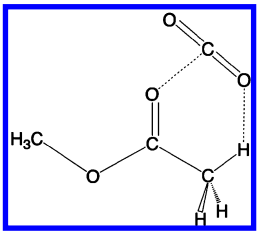

Interestingly, ab initio calculations performed in this work for the methyl acetate−CO_2 complex at the MP2[62] level with the aug-cc-pVDZ basis set show that the global minimum does not correspond to the structure drawn in Scheme 1. Actually, at this computational level, there is another energy minimum corresponding to an out-of-plane configuration (Figure 13). Our computed interaction energy for this structure is −3.97 kcal/mol and it lies 0.3 kcal/mol below the planar one. The optimized geometry exhibits a cyclic type structure involving two C···O interactions at about 3 Å. Though a more detailed investigation will be necessary to better understand the intermolecular interactions involved, the ab initio results point toward the $O\cdots C_{solvent}$ interaction being the most important one in the complex, and thus they support the absence of a well-defined $H\cdots O_{solvent}$ peak in the RDFs derived from our simulations.

IV. CONCLUSIONS

The supramolecular chemistry of cyclodextrins in supercritical carbon dioxide has not been quite developed, though it may have many applications, particularly in the context of green chemistry and of pharmaceutical technologies. We have reported in this paper the first molecular dynamics simulations of a prototypical compound, the peracetylated β-CD, in $scCO_2$, and we have analyzed the main structural and dynamical properties of the system in this solvent.

Our results support the experimental suggestion of a self-closure of the molecular cavity. More precisely, they show that self-closure can be induced directly or indirectly by a change in the conformation of one pyranose unit (from chair to skew) and that it can occur on both the wide and narrow CD sides. Indeed, the cavity fluctuates between open, closed, and partially closed shapes and not surprisingly it exhibits a small (time-averaged) solvent accessibility. It is worth noting that the number of observed self-closure events along the 10 ns trajectory is rather limited, and hence, reaching definite statistical averages will require carrying out longer simulations. Nevertheless, from the present study, one can expect the formation of host−guest complexes involving peracetylated β-CD in $scCO_2$ to be much less favorable than the equivalent process in aqueous solution with N-β-CD, as preliminary measurements have pointed out.[30−32] Finally, the results presented herein highlight the role of dynamical effects in

dx.doi.org/10.1021/jp3001064 | J. Phys. Chem. B 2012, 116, 3982−3990

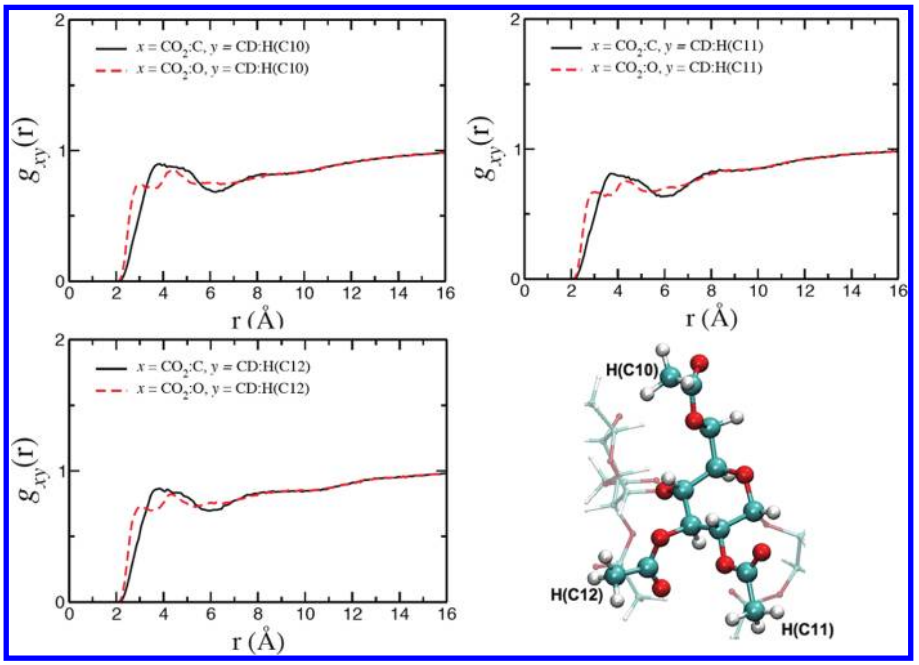

Figure 12. Solute−solvent radial distribution function for the C and O atoms of the solvent around the methyl H atoms (acetyl groups) on the narrow (H attached to C10) and on the wide (H attached to C11 and C12) side of the PA-β-CD in $scCO_2$.

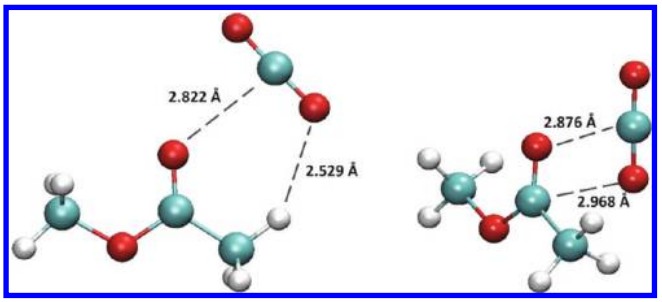

Figure 13. Fully optimized structures of the methyl acetate−CO_2 complex at the MP2/aug-cc-pvDZ level. The planar structure (left) is very close to that reported before.[61] The out-of-plane structure (right) is described here for the first time and has been found to lie 0.3 kcal/mol below the planar one.

$scCO_2$ so that the structural and inclusion properties of PA-β-CD are probably quite dependent on temperature and pressure conditions. This issue will need to be addressed in further experimental and theoretical work.

■ ASSOCIATED CONTENT

Supporting Information

Full refs 45 and 51. Atomic charges used in the force field. This material is available free of charge via the Internet at http://pubs.acs.org.

■ AUTHOR INFORMATION

Corresponding Author

*E-mail: Francesca.Ingrosso@uhp-nancy.fr (F.I.); Manuel.Ruiz@uhp-nancy.fr (M.F.R.).

Notes

The authors declare no competing financial interest.

■ ACKNOWLEDGMENTS

Financial support by the French National Research Agency (CREAM project, ref. ANR-09-BLAN-0180-01) and computational facilities by the CINES (project lct2550) are gratefully acknowledged. The authors thank Prof. Alain Marsura for interesting discussions.

■ REFERENCES

(1) Dodziuk, H. *Cyclodextrins and their complexes. Chemistry, analytical methods, applications*; Wiely-VCH Verlag GmbH & Co. KGaA: Weinheim, Germany, 2006.
(2) Del Valle, E. M. M. *Process Biochem.* **2004**, *39*, 1033−1046.
(3) Challa, R.; Ahuja, A.; Ali, J.; Khar, R. K. *AAPS PharmSciTech* **2005**, *6*, 329−357.
(4) Brewster, M. E.; Loftsson, T. *Adv. Drug Delivery Rev.* **2007**, *59*, 645−666.
(5) Uekama, K.; Hirayama, F.; Irie, T. *Chem. Rev.* **1998**, *98*, 2045−2076.
(6) Szejtli, J. *Chem. Rev.* **1998**, *98*, 1743−1754.
(7) Uekama, K.; Otagiri, M. *Crit. Rev. Ther. Drug Carrier Syst.* **1987**, *3*, 1−40.
(8) Stella, V. J.; Rajewski, R. A. *Pharm. Res.* **1997**, *14*, 556−567.
(9) Loftsson, T.; Brewster, M. E. *J. Pharm. Sci.* **1996**, *85*, 1017−1025.
(10) Rajewski, R. A.; Stella, V. J. *J. Pharm. Sci.* **1996**, *85*, 1142−1169.
(11) Sauceau, M.; Rodier, E.; Fages, J. *J. Supercrit. Fluids* **2008**, *47*, 326−332.
(12) Eckert, C. A.; Knutson, B. L.; Debenedetti, P. G. *Nature* **1996**, *383*, 313−318.
(13) Wells, S. L.; Desimone, J. *Angew. Chem., Int. Ed.* **2001**, *40*, 518−527.
(14) Mesiano, A. J.; Beckman, E. J.; Russell, A. J. *Chem. Rev.* **1999**, *99*, 623−634.
(15) Jessop, P. G.; Leitner, W. *Chemical Synthesis using Supercritical fluids*; Wiely-VCH Verlag GmbH & Co. KGaA: Weinheim, Germany, 1999.
(16) Raveendran, P.; Blatchford, M. A.; Hurrey, M. L.; White, P. S.; Wallen, S. L. *Green Chem.* **2005**, *7*, 129−131.
(17) Fages, J.; Lochard, H.; Letourneau, J. J.; Sauceau, M.; Rodier, E. *Powder Technol.* **2004**, *141*, 219−226.
(18) Foster, N.; Mammucari, R.; Dehghani, F.; Barrett, A.; Bezanehtak, K.; Coen, E.; Combes, G.; Meure, L.; Ng, A.; Regtop, H. L.; Tandya, A. *Ind. Eng. Chem. Res.* **2003**, *42*, 6476−6493.

(19) Scondo, A.; Dumarcay, F.; Marsura, A.; Barth, D. *J. Supercrit. Fluids* **2010**, *53*, 60−63.
(20) Scondo, A.; Dumarcay-Charbonnier, F.; Marsura, A.; Barth, D. *J. Supercrit. Fluids* **2009**, *48*, 41−47.
(21) Potluri, V. K.; Xu, J.; Enick, R.; Beckman, E.; Hamilton, A. D. *Org. Lett.* **2002**, *4*, 2333−2335.
(22) Potluri, V. K.; Hamilton, A. D.; Karanikas, C. F.; Bane, S. E.; Xu, J.; Beckman, E. J.; Enick, R. M. *Fluid Phase Equilib.* **2003**, *211*, 211−217.
(23) Raveendran, P.; Wallen, S. L. *J. Am. Chem. Soc.* **2002**, *124*, 7274−7275.
(24) Kazarian, S. G.; Vincent, M. F.; Bright, F. V.; Liotta, C. L.; Eckert, C. A. *J. Am. Chem. Soc.* **1996**, *118*, 1729−1736.
(25) Sarbu, T.; Styranec, T.; Beckman, E. J. *Nature* **2000**, *405*, 165−168.
(26) Añibarro, M.; Gessler, K.; Usón, I.; Sheldrick, G. M.; Harata, K.; Uekama, K.; Hirayama, F.; Abe, Y.; Saenger, W. *J. Am. Chem. Soc.* **2001**, *123*, 11854−11862.
(27) Uccello-Barretta, G.; Sicoli, G.; Balzano, F.; Salvadori, P. *Carbohydr. Res.* **2003**, *338*, 1103−1107.
(28) Caira, M. R.; Bettinetti, G.; Sorrenti, M.; Catenacci, L.; Cruickshank, D.; Davies, K. *Chem. Commun.* **2007**, 1221−1223.
(29) Steiner, T.; Saenger, W. *Angew. Chem., Int. Ed.* **1998**, *37*, 3404−3407.
(30) Galia, A.; Navarre, E. C.; Scialdone, O.; Ferreira, M.; Filardo, G.; Tilloy, S.; Monflier, E. *J. Phys. Chem. B* **2007**, *111*, 2573−2578.
(31) Galia, A.; Navarre, E. C.; Scialdone, O.; Filardo, G.; Monflier, E. *J. Supercrit. Fluids* **2009**, *49*, 154−160.
(32) Ivanova, G. I.; Vão, E. R.; Temtem, M.; Aguiar-Ricardo, A.; Casimiro, T.; Cabrita, E. J. *Magn. Reson. Chem.* **2009**, *47*, 133−141.
(33) Sayede, A. D.; Ponchel, A.; Filardo, G.; Galia, A.; Monflier, E. *J. Mol. Struct.: THEOCHEM* **2006**, *777*, 99−106.
(34) Csonka, G. I.; Ángyán, J. G. *J. Mol. Struct.: THEOCHEM* **1997**, *393*, 31−38.
(35) Bernal-Uruchurtu, M. I.; Martins-Costa, M. T. C.; Millot, C.; Ruiz-López, M. F. *J. Comput. Chem.* **2000**, *21*, 572−581.
(36) Bernal-Uruchurtu, M. I.; Ruiz-López, M. F. *Chem. Phys. Lett.* **2000**, *330*, 118−124.
(37) Casadesús, R.; Moreno, M.; González-Lafont, A.; Lluch, J. M.; Repasky, M. P. *J. Comput. Chem.* **2004**, *25*, 99−105.
(38) Klepko, V.; Ryabov, S.; Kercha, Y.; Bulavin, L.; Bila, R.; Slisenko, V.; Vasilkevich, O.; Krotenko, V. *J. Mol. Liq.* **2005**, *120*, 67−69.
(39) Georg, H. C.; Coutinho, K.; Canuto, S. *Chem. Phys. Lett.* **2005**, *413*, 16−21.
(40) Lawtrakul, L.; Viernstein, H.; Wolschann, P. *Int. J. Pharm.* **2003**, *256*, 33−41.
(41) Winkler, R. G.; Fioravanti, S.; Ciccotti, G.; Margheritis, C.; Villa, M. *J. Comput.-Aided Mol. Des.* **2000**, *14*, 659−667.
(42) Koehler, J. E.; Saenger, W.; van Gunsteren, W. F. *J. Biomol. Struct. Dyn.* **1988**, *6*, 181−198.
(43) Koehler, J. E. H.; Saenger, W.; van Gunsteren, W. F. *Eur. Biophys. J.* **1987**, *15*, 211−224.
(44) Heine, T.; Dos Santos, H. F.; Patchkovskii, S.; Duarte, H. A. *J. Phys. Chem. A* **2007**, *111*, 5648−5654.
(45) Case, D. A., et al. *AMBER 9*; University of California: San Francisco, 2006.
(46) Harris, J. G.; Yung, K. H. *J. Phys. Chem.* **1995**, *99*, 12021−12024.
(47) Basma, M.; Sundara, S.; Çalgan, D.; Vernali, T.; Woods, R. J. *J. Comput. Chem.* **2001**, *22*, 1125−1137.
(48) Woods, R. J.; Dwek, R. A.; Edge, C. J.; Fraser-Reid, B. *J. Phys. Chem.* **1995**, *99*, 3832−3846.
(49) Bayly, C. I.; Cieplak, P.; Cornell, W.; Kollman, P. A. *J. Phys. Chem.* **1993**, *97*, 10269−10280.
(50) Cornell, W. D.; Cieplak, P.; Bayly, C. I.; Gould, I. R.; Merz, K. M.; Ferguson, D. M.; Spellmeyer, D. C.; Fox, T.; Caldwell, J. W.; Kollman, P. A. *J. Am. Chem. Soc.* **1995**, *117*, 5179−5197.
(51) Frisch, M. J., et al. *Gaussian 09, Revision B.01*; Gaussian, Inc.: Wallingford, CT, 2010.
(52) Allen, M. P.; Tildesley, D. J. *Computer simulation of liquids*; Oxford University Press: Oxford, UK, 1987.
(53) Yeguas, V.; Altarsha, M.; Monard, G.; López, R.; Ruiz-López, M. F. *J. Phys. Chem. A* **2011**, *115*, 11810−11817.
(54) Duan, Y.; Wu, C.; Chowdhury, S.; Lee, M. C.; Xiong, G.; Zhang, W.; Yang, R.; Cieplak, P.; Luo, R.; Lee, T.; Caldwell, J.; Wang, J.; Kollman, P. *J. Comput. Chem.* **2003**, *24*, 1999−2012.
(55) Jorgensen, W. L.; Chandrasekhar, J.; Madura, J. D.; Impey, R. W.; Klein, M. L. *J. Chem. Phys.* **1983**, *79*, 926−935.
(56) Essmann, U.; Perera, L.; Berkowitz, M. L.; Darden, T.; Lee, H.; Pedersen, L. G. *J. Chem. Phys.* **1995**, *103*, 8577−8593.
(57) Humphrey, W.; Dalke, A.; Schulten, K. *J. Mol. Graphics* **1996**, *14*, 33−38.
(58) DeLano, W. L. *The PyMOL Molecular Graphics System, Version 1.2r1*; DeLano Scientific: San Carlos, CA, 2002.
(59) Biarnés, X.; Ardèvol, A.; Planas, A.; Rovira, C.; Laio, A.; Parrinello, M. *J. Am. Chem. Soc.* **2007**, *129*, 10686−10693.
(60) Raveendran, P.; Wallen, S. L. *J. Am. Chem. Soc.* **2002**, *124*, 12590−12599.
(61) Kim, K. H.; Kim, Y. *J. Phys. Chem. A* **2008**, *112*, 1596−1603.
(62) Møller, C.; Plesset, M. S. *Phys. Rev.* **1934**, *46*, 618−622.